

The Doubly Base-Stabilized Diborane(4) [HB(μ -hpp)]₂ (hpp = 1,3,4,6,7,8-hexahydro-2*H*-pyrimido[1,2-*a*]pyrimidine): Synthesis by Catalytic Dehydrogenation and Reactions with S₈ and Disulfides

Nikola Schulenberg,^[a] Oxana Ciobanu,^[a] Elisabeth Kaifer,^[a] Hubert Wadepohl,^[a] and Hans-Jörg Himmel^{*[a]}

Keywords: Boron / Hydrides / Sulfur / Guanidines

In this work we report on new experiments on the catalytic dehydrogenation of [H₂B(μ -hpp)]₂ leading to the doubly base-stabilized diborane(4) [HB(μ -hpp)]₂ featuring two hpp bridges (hpp = 1,3,4,6,7,8-hexahydro-2*H*-pyrimido[1,2-*a*]pyrimidine) under mild conditions. Several dehydrogenation (pre)catalysts were tested. The best one turned out to be Ru₃(CO)₁₂, allowing quantitative dehydrogenation already at 60 °C. Subsequently we subjected [HB(μ -hpp)]₂ to reactions

with S₈ and disulfides (Ph₂S₂ and Bn₂S₂, Bn = benzyl). Reaction with S₈ leads to oxidative insertion of one sulfur atom into the B–B bond and formation of [HB(μ -hpp)]₂(μ -S). In the case of disulfides, substitution reactions leading to the doubly base-stabilized diborane(4) species [RSB(μ -hpp)]₂ and HB(μ -hpp)₂BSR (R = Ph or Bn) compete with sulfuration again leading to [HB(μ -hpp)]₂(μ -S).

Introduction

Boron chemistry has regained considerable interest in recent years due to a series of exciting new discoveries. Hence a first neutral compound with a (base-stabilized) B=B bond was published by Robinson et al.^[1,2] Segawa, Yamashita and Nozaki reported on the synthesis and characterization of a first boron compound in which the boron center is nucleophilic (e. g., allowing nucleophilic attack on benzaldehyde).^[3,4] Braunschweig et al. stabilized a “ π -boryl anion” with the aid of an N-heterocyclic carbene.^[5,6] A number of complexes with borane, boryl, borylene and also boride ligands were synthesized, showing exciting electronic properties and a great potential for several applications.^[7] For example, boryl ligands were intensively applied in metal-catalysed borylation reactions.^[8] Recently even a first oxoboryl complex has been synthesized.^[9] Moreover, molecular boron compounds are of interest for hydrogen storage and as hydrogen transfer reagents. Hence catalytic dehydrogenation of amine borane (H₃N·BH₃), featuring a high hydrogen storage capacity (theoretically as high as 19.6% if all six hydrogen atoms are summed up), is currently studied intensively.^[10] Frustrated Lewis pairs (FLPs) containing boron as Lewis acidic site were demonstrated to activate small molecules and notably react reversibly with H₂.^[11,12] With

some relevance to this work the heterolytic cleavage of disulfides by FLPs was recently studied.^[13]

Recently we reported the synthesis of new doubly base-stabilized diborane(4) hydride species featuring bridging bicyclic guanidinate ligands.^[14–16] Hence [HB(μ -hpp)]₂ can be synthesized by thermal (catalytic) dehydrogenation of the adduct hppH·BH₃. So far we used for this purpose the complex [Rh(1,5-cod)(μ -Cl)]₂ as pre-catalyst and 110 °C.^[16] In an alternative route the diborane(4) B₂Cl₂(NMe₂)₂ is brought to reaction either with the neutral bicyclic guanidine, e. g. hppH to give [(Me₂N(H))B(μ -hpp)]₂²⁺,^[17,18] or with a Li salt such as hppLi to give the extremely unstable neutral [(Me₂N)B(μ -hpp)]₂, which is highly amenable to protonation at the NMe₂ groups.^[19] These doubly base-stabilized diborane(4) species exhibit a rich chemistry which we only just started to explore. Our work is motivated by a simple structure–reactivity concept. Hence the reactivity can be effectively controlled by the ring sizes of the guanidinate (see below),^[20] and also of course by the group 13 element used.^[21,22]

Results and Discussion

In the following we first discuss some new experiments on the catalytic dehydrogenation leading to the doubly base-stabilized diborane(4) [HB(μ -hpp)]₂ and quantum chemical calculations on the thermodynamics for hydrogenation of this and related systems. Then reactions of [HB(μ -hpp)]₂ with elemental sulfur and two disulfides (diphenyl disulfide, Ph₂S₂, and dibenzyl disulfide, Bn₂S₂) will be analysed.

[a] Anorganisch-Chemisches Institut, Ruprecht-Karls-Universität Heidelberg, Im Neuenheimer Feld 270, 69120 Heidelberg, Germany
Fax: +49-6221-545707

E-mail: hans-jorg.himmel@aci.uni-heidelberg.de
Supporting information for this article is available on the WWW under <http://dx.doi.org/10.1002/ejic.201000637>.

Dehydrogenation Reactions

In Figure 1 the gas-phase ΔG^0 value calculated for hydrogenation of several doubly base-stabilized diborane(4) species of the general formula $[\text{HB}(\mu\text{-guanidinate})]_2$ to give $[\text{H}_2\text{B}(\mu\text{-guanidinate})]_2$ is plotted as a function of the bite angle N–C–N of the bicyclic guanidinate in the product. All bicyclic guanidinate considered in this plot were already synthesized (see ref.^[23] for tbo and tbn, and ref.^[24] for tbd and tbu). Larger bite angles, which can simply be realized by choice of smaller ring sizes of the guanidinate bicycles, lead to a decrease of the ΔG^0 value for hydrogenation (the result of a linear fit is included in Figure 1). Thus it should be possible to tune the system to achieve optimal thermodynamic properties for reversibility ($\Delta G \approx 0 \text{ kJ mol}^{-1}$). Reversible oxidative addition reactions are then possible if the reaction barrier can be controlled by the aid of a catalyst.^[25] We showed in the past that the reverse reaction, dehydrogenation of $[\text{H}_2\text{B}(\mu\text{-hpp})]_2$ to give $[\text{HB}(\mu\text{-hpp})]_2$, can be achieved quantitatively in the presence of $[\text{Rh}(1,5\text{-cod})(\mu\text{-Cl})]_2$ as pre-catalyst in toluene solutions at 110 °C. This reaction is mildly exergonic at standard conditions ($\Delta G^0 = -30 \text{ kJ mol}^{-1}$). The same complex was shown to be a pre-catalyst^[26] for dehydrogenation of the amine boranes $\text{H}_3\text{N}\cdot\text{BH}_3$, $\text{H}(1,4\text{-C}_4\text{H}_8)\text{N}\cdot\text{BH}_2$, $\text{HMe}(\text{PhCH}_2)\text{N}\cdot\text{BH}_3$, $\text{H}_2\text{MeN}\cdot\text{BH}_3$, $\text{HMe}_2\text{N}\cdot\text{BH}_3$, $\text{H}_2\text{PhN}\cdot\text{BH}_3$, and

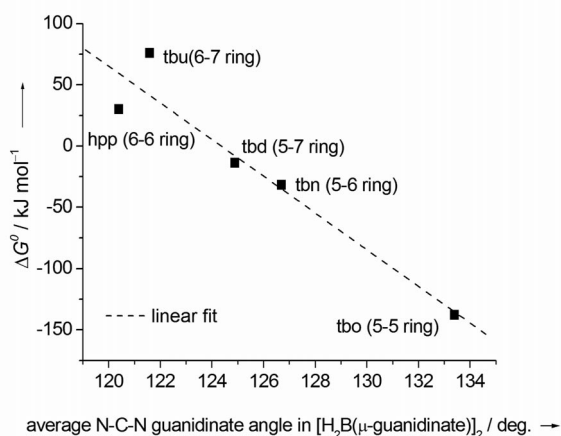


Figure 1. ΔG^0 for hydrogenation of $[\text{HB}(\mu\text{-guanidinate})]_2$ species as a function of the N–C–N bite angle of the bicyclic guanidinate in the hydrogenation product $[\text{H}_2\text{B}(\mu\text{-guanidinate})]_2$.

Table 1. Results of the catalytic dehydrogenation of $[\text{H}_2\text{B}(\mu\text{-hpp})]_2$.^[a]

Catalyst (mol-%)	Conditions for quantitative reaction ^[a]	Product
$[\text{Rh}(1,5\text{-cod})(\mu\text{-Cl})]_2$ (2%)	43 h, 115 °C, toluene	$[\text{HB}(\mu\text{-hpp})]_2$
$\text{Ru}_3(\text{CO})_{12}$ (10%)	12 h, 60 °C, toluene	$[\text{HB}(\mu\text{-hpp})]_2$
$\text{Ru}_3(\text{CO})_{12}$ (10%)	7 h, 80 °C, toluene	$[\text{HB}(\mu\text{-hpp})]_2$
Cp_2Ti (2%)	8 h, 80 °C, toluene	no reaction
$\text{Co}_2(\text{CO})_8$ (2%)	6 h, 80 °C, acetonitrile	–/–
$\text{Ni}(\text{PPh}_3)_4$ (2%)	72 h, 80 °C, toluene	–/–
$\text{Ni}(1,5\text{-cod})_2$, 2 Enders' NHC (5%)	65 h, 80 °C, acetonitrile	–/–
$\text{Ni}(1,5\text{-cod})_2$, 2 Enders' NHC (5%)	96 h, 110 °C, toluene	–/–
$(\text{C}_2\text{H}_4)\text{Pt}[\text{P}(\text{C}_6\text{H}_5)_3]_2$ (10%)	65 h, 80 °C, acetonitrile	–/–
Pd/C (2%)	72 h, 80 °C, toluene	–/–

[a] NMR experiments using 4 mg (0.013 mmol) of $[\text{H}_2\text{B}(\mu\text{-hpp})]_2$.

$\text{HiPr}_2\text{N}\cdot\text{BH}_3$ (at temperatures in the range 25 °C to 45 °C).^[27] Dehydrogenation starts after an induction period, during which a black suspension is formed.

In the hope to find catalysts which allow dehydrogenation at lower temperatures, we tested some other potential catalysts, the results are summarized in Table 1. Only temperatures of 80 °C or lower were considered. Most of the complexes included in Table 1 were already applied for dehydrogenation of amine boranes. Thus already in 1989, $\text{Ru}_3(\text{CO})_{12}$ was claimed to catalyse dehydrogenation of $\text{H}_3\text{N}\cdot\text{BH}_3$ and $\text{Me}_3\text{N}\cdot\text{BH}_3$ at 60 °C.^[28] In our experiments this carbonyl turned out to be a good pre-catalyst for dehydrogenation of $[\text{H}_2\text{B}(\mu\text{-hpp})]_2$. Directly upon addition of $\text{Ru}_3(\text{CO})_{12}$ to a toluene solution of the hydride the reaction mixture turned to a brownish colour, indicating decomposition of the pre-catalyst and heterogeneous catalytic conditions. Clean dehydrogenation to give $[\text{HB}(\mu\text{-hpp})]_2$ already occurs at 60 °C, and is completed in not more than 12 h [for addition of 10% of the $\text{Ru}_3(\text{CO})_{12}$ complex].^[29] The time needed for quantitative dehydrogenation can be further reduced to 7 h by increasing the temperature to 80 °C. Figure 2 shows the NMR spectra and the dehydrogenation kinetics at this temperature. The spectra indicate that dehydrogenation proceeds cleanly to give $[\text{HB}(\mu\text{-hpp})]_2$ as the single product. To determine the concentration of starting material and product, the integrals of the marked NMR signals were calculated. Based on the assumption that the sum of both integrals is constant, the rate of product formation appears to be exponential, in agreement with first-order kinetics. From a linear fit, as provided in Figure 2, k_{obs} and $t_{1/2}$ values of 0.0033 min^{-1} and 210 min, respectively, were deduced.

The dicarbene complex formed in situ from $\text{Ni}(1,5\text{-cod})_2$ and two equivalents of Ender's carbene (1,3,4-triphenyl-4,5-dihydro-1H-1,2,4-triazol-5-ylidene) was shown to dehydrogenate $\text{H}_3\text{N}\cdot\text{BH}_3$ at 60 °C in 3 h (for addition of 9% of the Ni catalyst),^[30,31] releasing 2.5 equiv. H_2 and yielding polyborazylene (and maybe other products in addition). Interestingly, this complex turned out to be inactive in the case of $[\text{H}_2\text{B}(\mu\text{-hpp})]_2$. No catalytic activity up to 80 °C was also found for Pd/C , $\text{Ni}(\text{PPh}_3)_4$, $\text{Co}_2(\text{CO})_8$ and $[(\text{C}_2\text{H}_4)\text{Pt}(\text{PPh}_3)_2]$. In the case of Cp_2Ti , catalytic activity was previously found at 110 °C. However, at 80 °C no dehydrogenation product of $[\text{H}_2\text{B}(\mu\text{-hpp})]_2$ was observed.

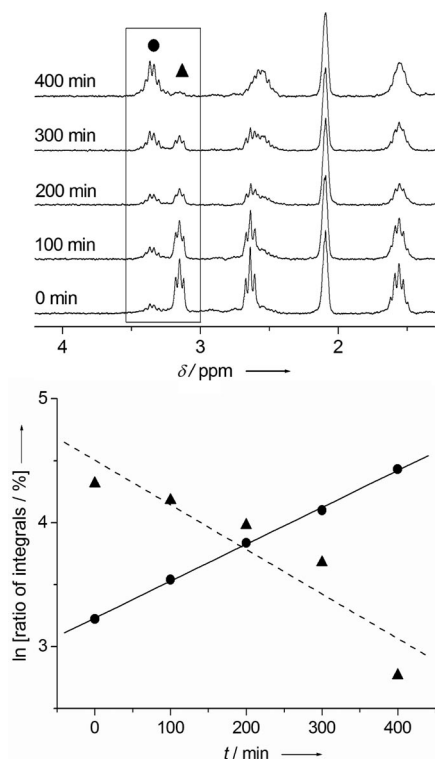


Figure 2. ^1H NMR spectra for the dehydrogenation of $[\text{H}_2\text{B}(\mu\text{-hpp})]_2$ to give the doubly base-stabilized diborane(4) $[\text{HB}(\mu\text{-hpp})]_2$, catalysed by $\text{Ru}_3(\text{CO})_{12}$ at 80°C in toluene solutions. Diagrams of the kinetic studies. The dashed and solid lines result from linear fits.

Reaction with Elemental Sulfur

Next we discuss the results of the reaction between $[\text{HB}(\mu\text{-hpp})]_2$ and S_8 . Addition of toluene to a solid mixture of $[\text{HB}(\mu\text{-hpp})]_2$ and S_8 at room temp. resulted in an intensely coloured solution. At the beginning it was purple, then slowly turned brown at room temp. (see the photographs of the solution at various stages of the reaction provided in the Supporting Information), finally the colour changed to turquoise upon heating of the reaction mixture to 90°C . The product precipitated upon cooling and was re-crystallized from toluene to give colourless crystals. The ^{11}B NMR spectrum of the product (in CD_3CN) displayed a sharp doublet centered at -1.98 ppm indicating the presence of B–H groups ($^1J_{\text{B-H}} = 114.1$ Hz) and tetra-coordinated boron atoms. For comparison, in the case of $[\text{H}_2\text{B}(\mu\text{-hpp})]_2$ (dissolved in toluene), $[\text{H}_2\text{B}(\mu\text{-tbo})]_2$ and $[\text{H}_2\text{B}(\mu\text{-tbn})]_2$ (dissolved in benzene), triplets centered at -2.30 , -10.81 and -5.73 (isomer in which each boron atom is attached to a five- and a six-membered ring) as well as $-4.32/-7.41$ ppm (isomer in which one boron is attached to two five-membered rings and the other to two six-membered rings), respectively, were found in the ^{11}B NMR spectra.^[32,20] In the case of $[\{\text{HB}(\mu\text{-hpp})\}_2(\mu\text{-H})]^+$ featuring a bridging hydride, the ^{11}B NMR shift measures -2.2 ppm.^[16] A strong band in the IR spectrum at 2359 cm^{-1} can be assigned to stretching modes $\nu(\text{B-H})$. In addition a strong band at 1559 cm^{-1} can be assigned to $\nu(\text{C=N})$ modes, di-

rectly indicating the presence of guanidinate ligands in the product. Thus the spectroscopic data point to oxidative insertion of sulfur into the B–B bond. Moreover the mass spectrometric data (EI) show an M^+ peak at $m/z = 332.2$, consistent with an overall product formula $\text{C}_{14}\text{H}_{26}\text{B}_2\text{N}_6\text{S}$ and insertion of one sulfur atom into the B–B bond. The molecular structure of this product, $[\text{HB}(\mu\text{-hpp})]_2(\mu\text{-S})$, was derived from X-ray diffraction experiments (see Figure 3). As expected, the sulfur atom bridges almost symmetrically the two B atoms [with B–S bond lengths of $188.6(2)$ and $189.4(2)$ pm]. The B \cdots B separation amounts to $258.0(1)$ pm, and is thus longer than that in $[\{\text{HB}(\mu\text{-hpp})\}_2(\mu\text{-H})]^+$ [$222.9(4)$ pm].^[16] As anticipated, the B–S–B bond angle of $86.07(9)^\circ$ is close to 90° (92.3° in H_2S). Interestingly, in other experiments the analogous compound $[\text{HB}(\mu\text{-hpp})]_2(\mu\text{-O})$ was crystallized in low yield, being the product of the reaction of $[\text{H}_2\text{B}(\mu\text{-hpp})]_2$ with traces of H_2O . In this case we were unable to isolate more than a few crystals suitable for X-ray diffraction, and therefore we can present the molecular structure of this species (see Figure 4), but no other analytical data. With $108.63(12)^\circ$ the B–O–B angle is significantly larger than the B–S–B angle, being close to the H–O–H bond angle of the H_2O molecule in the gas phase (104.5°).

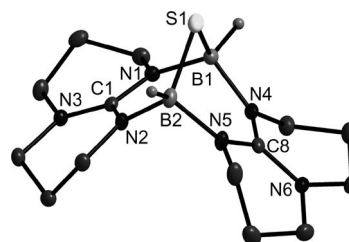


Figure 3. Molecular structure of $[\text{HB}(\mu\text{-hpp})]_2(\mu\text{-S})$. Ellipsoids drawn at the 50% probability level. Hydrogen atoms attached to carbon atoms were omitted for sake of clarity. Selected structural parameters (bond lengths in pm, bond angles in deg.): S–B1 $188.6(2)$, S–B2 $189.4(2)$, N1–B1 $156.5(2)$, N2–B2 $157.0(2)$, N4–B1 $157.7(2)$, N5–B2 $155.5(2)$, N1–C1 $134.6(2)$, N2–C1 $134.4(2)$, N3–C1 $135.8(2)$, N4–C8 $134.2(2)$, N5–C8 $133.8(2)$, N6–C8 $136.4(2)$, B1–S–B2 $86.07(9)$, N1–B1–N4 $110.79(14)$, N2–B2–N5 $109.76(15)$, N1–C1–N2 $118.74(15)$, N4–C8–N5 $119.87(15)$.

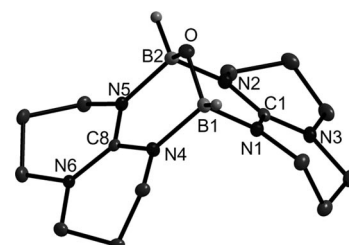
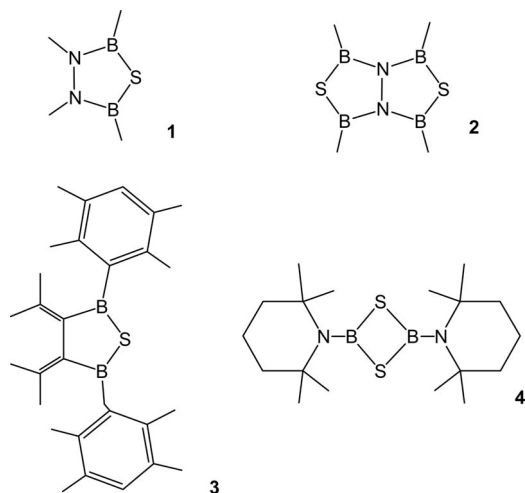


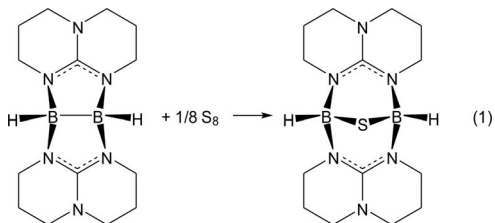
Figure 4. Molecular structure of $[\text{HB}(\mu\text{-hpp})]_2(\mu\text{-O})$. Ellipsoids drawn at the 50% probability level. Hydrogen atoms attached to carbon atoms were omitted for sake of clarity. Selected structural parameters (bond lengths in pm, bond angles in deg.): O–B1 $142.1(2)$, O–B2 $141.7(2)$, N1–B1 $158.6(2)$, N2–B2 $158.2(2)$, N4–B1 $157.9(2)$, N5–B2 $158.3(2)$, N1–C1 $134.05(19)$, N2–C1 $134.14(19)$, N3–C1 $136.00(18)$, N4–C8 $133.99(17)$, N5–C8 $134.07(18)$, N6–C8 $136.35(19)$, B1–O–B2 $108.63(12)$, N1–B1–N4 $109.14(11)$, N2–B2–N5 $108.54(12)$, N1–C1–N2 $118.57(12)$, N4–C8–N5 $118.14(13)$.

Heterocycles containing boron and sulfur atoms in the ring were studied intensively in the past. These studies mainly concentrated on tri-coordinated boron which can establish π -interactions.^[33] Four representative examples with the structural motif B–S–B, for which XRD data are available, are provided in Scheme 1. The B–S bond lengths in these molecules measure 181.0(10)/178.9(14) pm in **1**,^[34] 179.5(9)/180.6(9) pm in **2**,^[35] 182.4(2) pm in **3**,^[36] and 186.1(2) pm in **4**.^[37] As anticipated, these distances are shorter than the 188.6(2)/189.4(2) pm determined for [HB(μ -hpp)]₂(μ -S), for which boron–sulfur π -bonding is not significant (four-coordinate B atoms).



Scheme 1. Some known heterocycles containing the B–S–B structural motif.

Quantum chemical (DFT) calculations were carried out to obtain thermodynamic information about the reaction between [HB(μ -hpp)]₂ and S₈ (see Scheme 2). As anticipated, the reaction leading to B^{II} oxidation to B^{III} and reduction of elemental sulfur to S(-II) is significantly exergonic. The ΔE , ΔH^0 and ΔG^0 values were calculated to be –138, –132 and –121 kJ mol⁻¹, respectively.



Scheme 2. Sulfuration of the B–B bond in [HB(μ -hpp)]₂ by elemental sulfur.

The mechanism of this slow reaction involves several intermediates with relatively long life times, resulting from step-wise degradation of the S₈ ring as judged from the different colours observed at various stages of the reaction (see Supporting Information). In further experiments mixtures of [HB(μ -hpp)]₂ and S₈ were dissolved in toluene and the reaction followed by UV/Vis spectroscopy at 50 °C. In the first set of experiments one equivalent of [HB(μ -hpp)]₂ was treated with 1/8 equiv. of S₈. The UV/Vis spectra recorded

for this mixture are shown in Figure 5 (a). The spectrum recorded after 15 min contains two relatively broad absorptions centered at 504 and 618 nm. After 23 min, an intense blue colour was obtained and the band at 618 nm gained in intensity (see Figure 5, a). The extinction coefficient amounts to 5814 L mol⁻¹ cm⁻¹ at 50 °C based on the concentration of S₈. For longer reaction times the 618 nm band decreased again. In another set of experiments we used equimolar ratios of [HB(μ -hpp)]₂ and S₈. The UV/Vis spectra recorded in these experiments are shown in Figure 5 (b). In this case the band at 504 nm is more intense than that at 618 nm. The intensity of the 504 nm band reaches a maximum after 20 min and then decreases again. A brown colour results and the extinction coefficient at 504 nm is 1357 L mol⁻¹ cm⁻¹ at 50 °C based on the concentration of S₈. The spectra give useful information about the polysulfide ions present in the reaction mixture. There can be no doubt that S₈²⁻ is responsible for the band at 504 nm, a species that has been identified also as the first product of electrochemical reduction of S₈ in aprotic solvents.^[38,39] Addition of two more electrons to S₈²⁻ generates the unstable S₈⁴⁻, which dissociates to S₄²⁻. The two dianions S₄²⁻ and S₈²⁻ are in equilibrium with S₆²⁻, which itself dissociates to give S₃⁻. S₃⁻ is well known to exhibit a characteristic absorption at 618 nm and is responsible for the blue colour of electrochemically reduced sulfur in solution.^[39,40] It also is responsible for the blue colour of “Lapis lazuli”. Thus the two intermediates S₈²⁻ and S₃⁻ are involved in the reduction

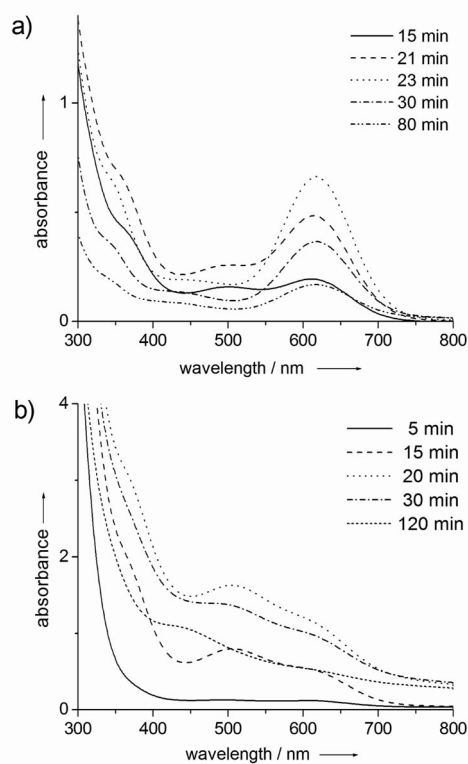


Figure 5. UV/Vis spectra recorded for the reaction between [HB(μ -hpp)]₂ and a) 1/8 equiv. of S₈, and b) 1 equiv. of S₈ in toluene solutions (see experimental details for more information).

of S_8 by $[\text{HB}(\mu\text{-hpp})]_2$. This might imply the presence of the dication $[\text{HB}(\mu\text{-hpp})]_2^{2+}$ as an intermediate, an extremely interesting species.

The reductive desulfuration of $[\text{HB}(\mu\text{-hpp})]_2(\mu\text{-S})$ was attempted by reaction with elemental zinc powder in boiling toluene solutions. However, no reaction was observed. Even after 58 h in boiling toluene, the ^1H and ^{11}B NMR spectra gave no sign of decomposition or reaction of boron hydride $[\text{HB}(\mu\text{-hpp})]_2(\mu\text{-S})$, underlining its remarkable stability.

Reactions with Disulfides

Reactions between $[\text{HB}(\mu\text{-hpp})]_2$ and Ph_2S_2 or Bn_2S_2 gave a mixture of three different products, namely the sulfuration product $[\text{HB}(\mu\text{-hpp})]_2(\mu\text{-S})$ and the products of substitution of one or both hydrides by thiolate (PhS or BnS). By variation of the conditions for crystallization, all these products can be isolated. We also were able to obtain larger quantities of clean product by crystal picking. In this way, it was possible to collect almost all standard analytic data for the four species $[\text{PhSB}(\mu\text{-hpp})]_2$, $[\text{BnSB}(\mu\text{-hpp})]_2$, $\text{HB}(\mu\text{-hpp})_2\text{BSPH}$ and $\text{HB}(\mu\text{-hpp})_2\text{BSBn}$. However, because of the presence of a product mixture, the yields cannot be provided. Moreover, the product composition is very sensitive to small variations of the reaction conditions.

Figure 6 shows a representative $^{11}\text{B}\{^1\text{H}\}$ NMR spectrum of the reaction mixture obtained for reaction between $[\text{HB}(\mu\text{-hpp})]_2$ and Bn_2S_2 . For comparison, the $^{11}\text{B}\{^1\text{H}\}$ NMR spectra for clean solutions of $[\text{HB}(\mu\text{-hpp})]_2$, its sulfuration product $[\text{HB}(\mu\text{-hpp})]_2(\mu\text{-S})$, and the two substitution products $[\text{BnSB}(\mu\text{-hpp})]_2$ and $\text{HB}(\mu\text{-hpp})\text{BSBn}$ are also included. The signals are relatively broad for the B^{II} species, and sharp for the B^{III} compound $[\text{HB}(\mu\text{-hpp})]_2(\mu\text{-S})$. It can be seen that not a single product, but a mixture of the three products $[\text{HB}(\mu\text{-hpp})]_2(\mu\text{-S})$, $[\text{BnSB}(\mu\text{-hpp})]_2$ and $\text{HB}(\mu\text{-hpp})\text{BSBn}$ has been formed. Due to the broad signals and their overlapping, it turned out to be impossible to estimate

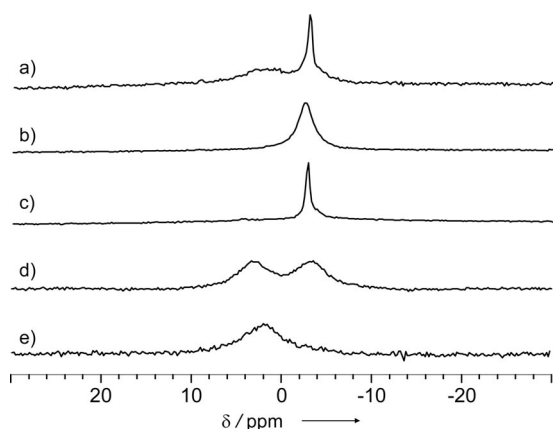


Figure 6. $^{11}\text{B}\{^1\text{H}\}$ NMR spectra recorded for the reaction between $[\text{HB}(\mu\text{-hpp})]_2$ and Bn_2S_2 after 3,5 h at 90 °C. The $^{11}\text{B}\{^1\text{H}\}$ NMR spectra recorded for b) $[\text{HB}(\mu\text{-hpp})]_2$, c) $[\text{HB}(\mu\text{-hpp})]_2(\mu\text{-S})$, d) $[\text{HB}(\mu\text{-hpp})_2\text{BSBn}]$, and e) $[\text{BnSB}(\mu\text{-hpp})]_2$ are also shown for comparison. All spectra were recorded at 64 MHz in CD_2Cl_2 except d) (in $[\text{D}_8]\text{THF}$) and e) (in C_6D_6).

the exact product composition in the solution. Nevertheless, from the inspection of the NMR spectroscopic data it can be concluded that ca. 50% sulfuration and ca. 50% substitution take place.

The molecular structures of the four new product compounds are displayed in Figures 7, 8, 9 and 10. With 172.2(7)/173.2(6), 173.2(3), 173.0(4) and 173.6(4) pm, respectively, the B–B bond lengths in $[\text{PhSB}(\mu\text{-hpp})]_2$, $[\text{BnSB}(\mu\text{-hpp})]_2$, $\text{HB}(\mu\text{-hpp})_2\text{BSPH}$ and $\text{HB}(\mu\text{-hpp})_2\text{BSBn}$ are similar and close to the 177.2(3) pm measured for $[\text{HB}(\mu\text{-hpp})]_2$. The B–S bond lengths in the disubstituted compounds $[\text{PhSB}(\mu\text{-hpp})]_2$ and $[\text{BnSB}(\mu\text{-hpp})]_2$ [193.9(5)/194.6(5) and 194.0(2)/191.5(2) pm] are in average slightly shorter than in the monosubstituted species $\text{HB}(\mu\text{-hpp})_2$ -

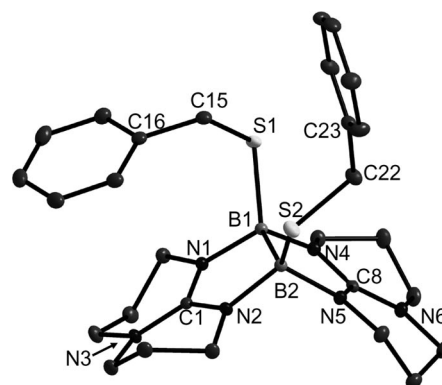


Figure 7. Molecular structure of $[\text{BnSB}(\mu\text{-hpp})]_2$. Ellipsoids drawn at the 50% probability level. Hydrogen atoms attached to carbon atoms were omitted for sake of clarity. Selected structural parameters (bond lengths in pm, bond angles in deg.): B1–B2 173.2(3), N1–B1 155.8(2), N2–B2 155.1(2), N4–B1 154.5(2), N5–B2 156.9(2), S1–B1 194.0(2), S2–B2 191.5(2), N1–C1 133.6(2), N2–C1 145.6(2), N3–C1 134.8(3), N4–C8 133.4(5), N5–C8 145.6(2), N6–C8 135.2(4), S1–C15 182.3(2), S2–C22 182.1(2), C15–C16 150.5(3), C22–C23 150.6(3), N1–B1–N4 111.56(14), N2–B2–N5 114.06(14), B1–B2–S2 127.35(13), B2–B1–S1 126.83(12), N1–C1–N2 115.63(2), N4–C8–N5 115.73(2), B1–S1–C15 103.36(9), B2–S2–C22 101.93(9), S1–B1–B2–S2 6.80(3).

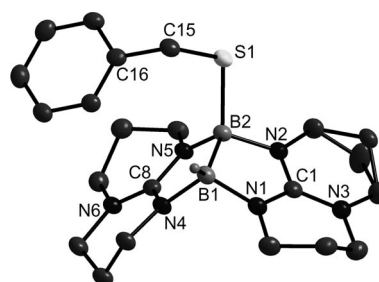


Figure 8. Molecular structure of $[\text{HB}(\mu\text{-hpp})_2\text{BSBn}]$. Ellipsoids drawn at the 50% probability level. Hydrogen atoms attached to carbon atoms were omitted for sake of clarity. Selected structural parameters (bond lengths in pm, bond angles in deg.): B1–B2 173.6(4), S–B2 194.1(3), S–C15 182.8(3), N1–B1 156.3(4), N2–B2 155.9(4), N4–B1 156.6(3), N5–B2 155.6(4), N1–C1 133.2(3), N2–C1 133.9(3), N3–C1 136.2(3), N4–C8 133.7(3), N5–C8 133.4(3), N6–C8 135.8(3), B1–B2–S 125.02(18), N1–B1–N4 112.9(2), N2–B2–N5 112.6(2), N1–C1–N2 115.6(2), N4–C8–N5 115.7(2), B2–S–C15 100.93(12).

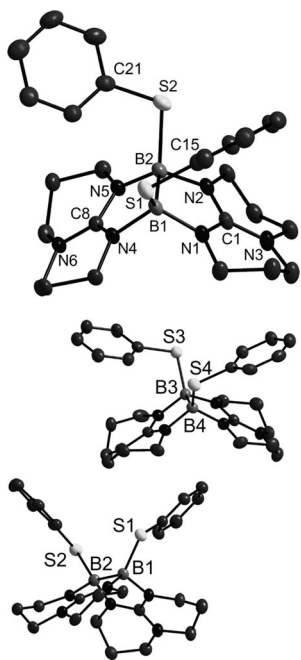


Figure 9. Molecular structure of $[\text{PhSB}(\mu\text{-hpp})]_2$. Ellipsoids drawn at the 50% probability level. Hydrogen atoms attached to carbon atoms were omitted for sake of clarity. Selected structural parameters (bond lengths in pm, bond angles in deg.): B1–B2 172.2(7), B3–B4 173.2(6), S1–B1 193.9(5), S2–B2 194.6(5), S3–B3 194.9(5), S4–B4 196.2(4), N1–B1 155.1(6), N2–B2 156.1(6), N4–B1 154.7(5), N5–B2 154.4(5), N1–C1 133.3(5), N2–C1 134.3(5), N3–C1 135.1(5), N4–C8 134.2(5), N5–C8 134.6(5), N6–C8 134.8(5), S1–C20 177.5(2), S2–C26 179.7(2), N1–B1–N4 113.9(3), N2–B2–N5 112.3(3), B2–B1–S1 127.6(3), B1–B2–S2 126.8(3), N1–C1–N2 116.0(4), N4–C8–N5 115.0(3), S1–B1–B2–S2 8.141(23).

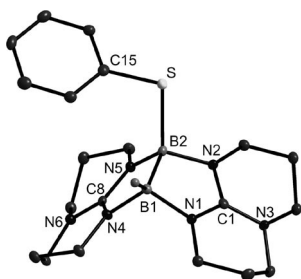


Figure 10. Molecular structure of $[\text{HB}(\mu\text{-hpp})_2\text{BSPH}]$. Ellipsoids drawn at the 50% probability level. Hydrogen atoms attached to carbon atoms omitted for sake of clarity. Selected structural parameters (bond lengths in pm, bond angles in deg.): B1–B2 173.0(4), S–B2 195.9(3), N1–B1 157.6(3), N2–B2 154.8(3), N4–B1 156.2(3), N5–B2 156.1(3), N1–C1 133.9(3), N2–C1 134.6(3), N3–C1 135.3(3), N4–C8 133.8(3), N5–C8 135.1(3), N6–C8 136.0(3), S–C15 176.8(2), B1–B2–S 128.97(16), N1–B1–N4 111.28(18), N2–B2–N5 112.86(18), N1–C1–N2 115.09(19), N4–C8–N5 115.67(18), B2–S–C15 103.30(11).

BSPH and $\text{HB}(\mu\text{-hpp})_2\text{SBn}$ [195.9(3) and 194.1(3) pm]. The B–B–S bond angles are very similar, all within the region 126–129°.

The reaction of $[\text{HB}(\mu\text{-hpp})]_2$ with R_2S_2 (R = Ph or Bn) presumably leads first to the product of oxidative addition, $[(\text{RS})(\text{H})\text{B}(\mu\text{-hpp})]_2$. Unfortunately it was not possible to isolate this intermediate, even when the reaction was carried

out at 0 °C. However, ^{11}B NMR spectra (C_7D_8 , 64 MHz) taken for reaction between $[\text{HB}(\mu\text{-hpp})]_2$ and 1 equiv. Bn_2S_2 at 40 °C in an ultrasonic bath gave some indication for an intermediate which might indeed be $[(\text{BnS})(\text{H})\text{B}(\mu\text{-hpp})]_2$ (see the NMR spectra in the Supporting Information). Hence in these experiments a doublet centered at $\delta = 4.97$ ppm ($^1J_{\text{BH}} = 112.5$ Hz) appeared which first grew in intensity, but decreased again in intensity with time, finally, for 52 h at 40 °C it almost completely disappeared. $[(\text{RS})(\text{H})\text{B}(\mu\text{-hpp})]_2$ might be responsible for this doublet. In addition, the broad signal at -1.19 ppm belonging to the starting material disappeared, and a doublet at -0.81 ppm ($^1J_{\text{BH}} = 114.5$ Hz) due to $[\text{HB}(\mu\text{-hpp})]_2(\mu\text{-S})$ increased in intensity. Quantum chemical calculations were carried out to shed light on the thermodynamic properties for the pathways leading to the products $\text{HB}(\mu\text{-hpp})_2\text{BSPH}$, $[(\text{PhS})\text{B}(\mu\text{-hpp})]_2$ and $[\text{HB}(\mu\text{-hpp})]_2(\mu\text{-S})$ via $[(\text{PhS})(\text{H})\text{B}(\mu\text{-hpp})]_2$ as common intermediate (see Figure 11). The formation of $[(\text{PhS})(\text{H})\text{B}(\mu\text{-hpp})]_2$ from $[\text{HB}(\mu\text{-hpp})]_2$ and Ph_2S_2 ($\Delta G^0 = -50$ kJ mol $^{-1}$), as well as the following elimination processes leading to the observed products are all exergonic reactions. The elimination of Ph_2S to give $[\text{HB}(\mu\text{-hpp})]_2(\mu\text{-S})$ is the most exergonic process, in line with the preferred formation of this product in the experiments. Interestingly, dehydrogenation of $[(\text{PhS})(\text{H})\text{B}(\mu\text{-hpp})]_2$ ($\Delta G^0 = -65$ kJ mol $^{-1}$) is significantly more exergonic than dehydrogenation of $[\text{H}_2\text{B}(\mu\text{-hpp})]_2$ ($\Delta G^0 = -30$ kJ mol $^{-1}$). The fairly large number of atoms in the involved species causes long computational times if transition states should be calculated. In preliminary calculations using H_2S_2 in place for Ph_2S_2 , we obtained a ΔG^0 value of -78 kJ mol $^{-1}$ for oxidative addition to give the intermediate species $[(\text{HS})(\text{H})\text{B}(\mu\text{-hpp})]_2$ (see Supporting Information). The reason for the significant discrepancy between this value and the value obtained for Ph_2S_2 (-50 kJ mol $^{-1}$) arises (at least partially) from the presence of S–H \cdots S hydrogen bonding in $[(\text{HS})(\text{H})\text{B}(\mu\text{-hpp})]_2$ (see Supporting Information). Reduction of the computational time for transition state calculations simply by replacement of the substituents by hydrogen atoms is therefore difficult. We have therefore set aside further calcula-

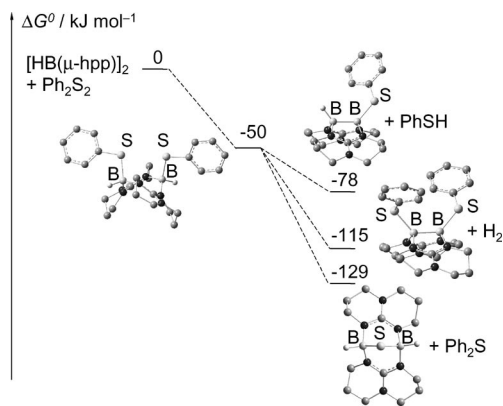


Figure 11. ΔG^0 values for the reaction between $[\text{HB}(\mu\text{-hpp})]_2$ and Ph_2S_2 , leading to the three observed products $[\text{HB}(\mu\text{-hpp})]_2(\mu\text{-S})$, $[\text{HB}(\mu\text{-hpp})\text{BSPH}]$ and $[\text{PhSB}(\mu\text{-hpp})]_2$ via $[(\text{PhS})(\text{H})\text{B}(\mu\text{-hpp})]_2$ as common intermediate.

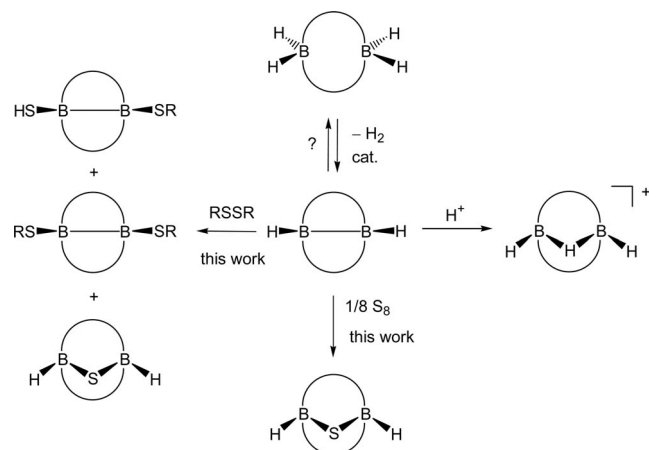
tions. The experiments indicate that the barriers for all three elimination reactions starting from the intermediate are in the same order.

Conclusions

The chemistry of the doubly base-stabilized diborane(4) species $[\text{HB}(\mu\text{-hpp})_2]$ (hpp = 1,3,4,6,7,8-hexahydro-2*H*-pyrimido[1,2-*a*]pyrimidine) is described. This boron hydride can be synthesized by catalytic dehydrogenation of the binuclear B^{III} hydride $[\text{H}_2\text{B}(\mu\text{-hpp})_2]$. The conditions and the catalyst for this reaction were optimized. Quantum chemical calculations analyse the thermodynamics for hydrogenation of $[\text{HB}(\mu\text{-hpp})_2]$ and analogous species with other bridging, bicyclic guanidinate substituents. These calculations support the assumption of an almost linear relationship between the standard Gibbs free energy for hydrogenation and the N–C–N bite angle of the guanidinate in the hydrogenated product. The main aim of future work will be the optimization of the conditions for (catalytic) hydrogenation of $[\text{HB}(\mu\text{-guanidinate})_2]$. They will concentrate on the 6–6 and 5–6 bicyclic guanidinate hpp and tbn as bridging substituents.

The oxidative sulfuration of $[\text{HB}(\mu\text{-hpp})_2]$ with S_8 leading to $[\text{HB}(\mu\text{-hpp})_2(\mu\text{-S})]$ is an example for oxidative insertion into the B–B bond. The reaction with the disulfides Ph_2S_2 and Bn_2S_2 leads to $[\text{HB}(\mu\text{-hpp})_2(\mu\text{-S})]$ as well as the substitution products $[\text{HB}(\mu\text{-hpp})_2\text{SR}]$ and $[\text{RS}(\mu\text{-hpp})_2]$ (R = Ph or Bn). All these products were structurally characterized. The experimental results together with quantum chemical calculations indicate that oxidative addition of the disulfide first leads to $[(\text{PhS})(\text{H})\text{B}(\mu\text{-hpp})_2]$, which acts as common intermediate on the way to all three products. We will extend our work to other disulfides, one of the aims being the synthesis of species of the general formula $[\text{RSB}(\mu\text{-hpp})_2]$ by avoiding the sulfuration pathway.

These species possibly find applications as oxidation-labile, chelating sulfur ligands. Scheme 3 summarizes the so far studied reactions of the doubly base-stabilized diborane(4) species $[\text{HB}(\mu\text{-hpp})_2]$.



Scheme 3. Reactivity of $[\text{HB}(\mu\text{-hpp})_2]$ (hpp is symbolized by a curved line connecting the two B atoms).

Experimental Details

General Procedures: All reactions were carried out under a dry argon atmosphere using standard Schlenk techniques. Solvents were dried with the appropriate drying agents, distilled and preserved over molecular sieves (4 Å) prior to use. The bicyclic guanidine hppH, dibenzyl disulfide and diphenyl disulfide were purchased from Aldrich. Sulfur was purchased from Grüssing. Infrared spectra were recorded using a BIORAD Excalibur FTS 3000. NMR spectra were recorded on a Bruker Avance II 400 or on a Bruker Avance DPX AC200. Elemental analyses were carried out at the Microanalytical Laboratory of the University of Heidelberg. EI mass spectra were obtained on a Finnigan MAT 8230 or on a JEOL JMS-700 instrument.

$[\text{HB}(\mu\text{-hpp})_2]$: A Schlenk flask, charged with hppH (2.51 g, 18.03 mmol), trimethylamine borane (1.32 g, 18.03 mmol), $[\text{Rh}(\text{1,5-cod})(\mu\text{-Cl})_2]$ (18 mg, 0.03 mmol) and toluene (75 mL) was heated to reflux for 65 h. The brown solution was filtered, concentrated and stored for several days at 3 °C to afford colourless crystals of the clean product in 61% yield (1.65 g, 5.51 mmol). ^1H NMR (200 MHz, C_6D_6): δ = 3.57–3.32 (m, 8 H, $\text{CH}_2\text{-N}$), 2.51–1.28 (m, 8 H, $\text{CH}_2\text{-N}$), 1.56–1.18 (m, 8 H, CH_2) ppm. ^{11}B NMR (128 MHz, C_6D_6): δ = –1.14 (br. s, BH) ppm. See ref. 16 for more analytical data.

$[\text{HB}(\mu\text{-hpp})_2(\mu\text{-S})]$: A Schlenk flask was charged with $[\text{HB}(\mu\text{-hpp})_2]$ (150 mg, 0.50 mmol) and sulfur (16 mg, 0.06 mmol). After addition of toluene (16 mL), the colour of the solution turned from purple to dark brown. By heating the solution to 90 °C, the colour of the solution turned into very dark turquoise, which lightens after a while. After heating for 16 h, the hot turquoise solution was filtered. By cooling to room temp., the product precipitated as a colourless solid. It was filtered and washed with *n*-hexane (1 × 2 mL). After drying in vacuo the product was achieved in 82% yield (136 mg, 0.41 mmol). Crystals suitable for x-ray diffraction were grown by recrystallisation from toluene solutions. $\text{C}_{14}\text{H}_{26}\text{B}_2\text{N}_6\text{S}$ (332.08): calcd. C 50.63, H 7.89, B 6.51, N 25.31, S 9.66; found C 50.24, H 7.94, N 25.03. ^1H NMR (600 MHz, CD_3CN): δ = 3.32–3.09 (m, 16 H, 2-H, 4-H), 1.82–1.77 (m, 8 H, 3-H) ppm. ^{13}C NMR (150 MHz, CD_3CN): δ = 152.8 (2 C, C-1), 49.0 (4 C, C-4/2), 48.1 (4 C, C-2/4), 23.7 (4 C, C-3) ppm. ^{11}B NMR (128 MHz, CD_3CN): δ = –1.98 [d, $^1J_{\text{BH}} = 114.1$ Hz, 2 B, B(H)S] ppm. MS (EI): m/z = 332.2 $[\text{C}_{14}\text{H}_{26}\text{B}_2\text{N}_6\text{S}]^+$. IR (KBr): $\tilde{\nu}$ = 2953 (m) (C–H val.), 2938 (m) (C–H val.), 2855 (s) (C–H val.), 2359 (s) (B–H val.), 1559 (s) (C=N val.), 1450 (m), 1397 (w), 1368 (w), 1312 (s), 1218 (s), 1173 (m), 1092 (s), 1048 (w) cm^{-1} . Crystal data for $[\text{HB}(\mu\text{-hpp})_2(\mu\text{-S})]$: $\text{C}_{14}\text{H}_{26}\text{B}_2\text{N}_6\text{S}$, $M_r = 332.09$, $0.25 \times 0.20 \times 0.20$ mm^3 , monoclinic, space group $P2_1/n$, $a = 13.183(3)$, $b = 8.076(2)$, $c = 16.637(3)$ Å, $\beta = 112.97(3)^\circ$. $V = 1630.80(6)$ Å³, $Z = 4$, $d_{\text{calc}} = 1.353$ Mg m^{-3} , Mo- K_α radiation (graphite-monochromated, $\lambda = 0.71073$ Å), $T = 100$ K, $\theta_{\text{range}} 1.69$ to 30.02° , reflections measd. 9345, indep. 4753, $R_{\text{int}} = 0.0206$, final R indices [$I > 2\sigma(I)$]: $R_1 = 0.0540$, $wR_2 = 0.1518$.

$[\text{PhSB}(\mu\text{-hpp})_2]$: A Schlenk flask containing $[\text{HB}(\mu\text{-hpp})_2]$ (150 mg, 0.5 mmol), diphenyl disulfide (109 mg, 0.5 mmol) and toluene (10 mL) was heated to reflux for 3 h. The solvent was removed and the yellow residue dissolved in dichloromethane (7 mL). The solution was overlaid with *n*-hexane and kept at 3 °C for 15 h. After this, the solvents were removed in vacuo again and the light-yellow residue was washed with tetrahydrofuran (2 × 7 mL). The white solid was dissolved in boiling acetonitrile and filtered hot. By cooling the filtrate to room temp. colourless crystals of $[\text{PhSB}(\mu\text{-hpp})_2]$ appeared. Unfortunately it was not possible to obtain enough crystalline material for an EA analysis. ^1H NMR

(400 MHz, CD₃CN): $\delta = 7.33$ (dd, $^3J_{\text{HH}} = 8.3$, $^4J_{\text{HH}} = 1.1$ Hz, 4 H, 16-H), 6.98 (dt, $^3J_{\text{HH}} = 8.0$, $^4J_{\text{HH}} = 1.6$ Hz, 4 H, 17-H), 6.85 (tt, $^3J_{\text{HH}} = 7.4$, $^4J_{\text{HH}} = 1.2$ Hz, 2 H, 18-H), 3.41–2.96 (m, 16 H, 2-H, 4-H), 1.76–1.46 (m, 8 H, 3-H) ppm. ¹³C NMR (100 MHz, CD₃CN): $\delta = 179.4$ (2 C, C-1), 143.8 (2 C, C-15), 132.1 (4 C, C-16), 128.0 (4 C, C-17), 122.7 (2 C, C-18), 47.9 (4 C, C-4/2), 40.9 (4 C, C-2/4), 22.9 (4 C, C-3) ppm. ¹¹B NMR (128 MHz, CD₃CN): $\delta = 2.38$ (br. s, 2 B, BS) ppm. MS (EI): $m/z = 516.3$ [C₂₆H₃₄B₂N₆S₂]⁺, 407.3 [C₂₀H₂₉B₂N₆S]⁺. HR-MS (EI): $m/z = 516.2471$ (27), 515.2485 (14), 407.2346 (100), 406.2383 (48). Crystal data for [PhSB(μ-hpp)]₂: C₂₆H₃₄B₂N₆S₂, $M_r = 516.34$, 0.30 × 0.30 × 0.20 mm³, monoclinic, space group $P2_1/c$, $a = 15.867(3)$, $b = 21.383(4)$, $c = 15.766(3)$ Å, $\beta = 103.86(3)^\circ$. $V = 5193.4$ Å³, $Z = 8$, $d_{\text{calc}} = 1.321$ Mg m⁻³, Mo- K_α radiation (graphite-monochromated, $\lambda = 0.71073$ Å), $T = 100$ K, $\theta_{\text{range}} 1.36$ to 27.93° , reflections measd. 40500, indep. 12198, $R_{\text{int}} = 0.1158$, final R indices [$I > 2\sigma(I)$]: $R_1 = 0.0784$, $wR_2 = 0.1573$.

HB(μ-hpp)₂BSPH: A Schlenk flask containing [HB(μ-hpp)]₂ (300 mg, 1.00 mmol), diphenyl disulfide (218 mg, 1.00 mmol) and toluene (20 mL) was heated to reflux for 3 h. By cooling to room temp., a white solid precipitated. The solution was filtered and the solid material was dissolved in boiling acetonitrile. Undissolved particles were filtered and by cooling the filtrate to room temp., colourless crystals of [HB(μ-hpp)₂BSPH] were obtained. The product is stable in dichloromethane only for a few hours. The yield was not determined. C₂₀H₃₀B₂N₆S (408.18): calcd. C 58.85, H 7.41, B 5.30, N 20.59, S 7.86; found C 59.07, H 7.41, N 19.97. ¹H NMR (400 MHz, CD₂Cl₂): $\delta = 7.18$ (dd, $^3J_{\text{HH}} = 8.1$, $^4J_{\text{HH}} = 1.0$ Hz, 2 H, 16-H), 7.00 (t, $^3J_{\text{HH}} = 7.8$ Hz, 2 H, 17-H), 6.84 (t, $^3J_{\text{HH}} = 7.4$ Hz, 1 H, 18-H), 3.45–2.96 (m, 16 H, CH₂-N), 1.95–1.59 (m, 8 H, C-CH₂-C) ppm. ¹³C NMR (100 MHz, CD₂Cl₂): $\delta = 156.3$ (2 C, C-1), 143.6 (1 C, C-15), 130.1 (2 C, C-16), 126.9 (2 C, C-17), 121.1 (1 C, C-18), 47.0 (2 C, CH₂-N), 46.8 (2 C, CH₂-N), 44.4 (2 C, CH₂-N), 40.1 (2 C, CH₂-N), 22.3 (4 C, C-3, C-6, C-10, C-13) ppm. ¹¹B NMR (128 MHz, CD₂Cl₂): $\delta = 2.38$ (br. s, 1 B, B-S), -2.38 (br. s, 1B, B-H) ppm. MS (EI): $m/z = 407.3$ [C₂₀H₂₉B₂N₆S]⁺. IR (KBr): $\tilde{\nu} = 3044$ (w) (C-H_{arom} val.), 2956 (m) (C-H_{aliph} val.), 2926 (m) (C-H_{aliph} val.), 2845 (s) (C-H_{aliph} val.) 2283 (s) (B-H val.), 1578 (s) (C=N val.), 1461 (m), 1397 (w), 1368 (w), 1313 (s), 1266 (s), 1261 (m), 1178 (w), 1092 (s), 1025 (s) cm⁻¹. Crystal data for [HB(μ-hpp)₂BSPH]: C₂₀H₃₀B₂N₆S, $M_r = 408.18$, 0.35 × 0.30 × 0.30 mm³, monoclinic, space group $P2(1)$, $a = 8.133(2)$, $b = 15.218(3)$, $c = 8.668(2)$ Å, $\beta = 106.38(3)^\circ$. $V = 1029.30$ Å³, $Z = 2$, $d_{\text{calc}} = 1.317$ Mg m⁻³, Mo- K_α radiation (graphite-monochromated, $\lambda = 0.71073$ Å), $T = 100$ K, $\theta_{\text{range}} 2.45$ to 27.46° , reflections measd. 4736, indep. 4717, $R_{\text{int}} = 0.0000$, final R indices [$I > 2\sigma(I)$]: $R_1 = 0.0447$, $wR_2 = 0.0837$.

[BnSB(μ-hpp)]₂: A Schlenk flask containing [HB(μ-hpp)]₂ (105 mg, 0.35 mmol), dibenzyl disulfide (173 mg, 0.70 mmol) and toluene (10 mL) was heated to reflux for 3.5 h. The solvent was removed, the oily residue co-evaporated with toluene (2 × 2 mL) and dried in vacuo for several hours to remove benzylthiole. The yellow oil was redissolved in toluene (6 mL) and overlaid with *n*-hexane (4 mL) to precipitate the by-products. After storage for 17 h at 3 °C a colourless non-crystalline solid appeared which was filtered. The filtrate was again overlaid with *n*-hexane. This procedure was repeated one more time. By storage at room temp. large yellow crystals of [BnSB(μ-hpp)]₂, suitable for x-ray diffraction were obtained. However, only small amounts can be isolated (see text). C₂₈H₃₈B₂N₆S₂ (544.39): calcd. C 61.78, H 7.04, B 3.97, N 15.44, S 11.78; found C 62.11, H 6.86, N 15.85. ¹H NMR (400 MHz, C₆D₆): $\delta = 7.84$ (dd, $^3J_{\text{HH}} = 8.2$, $^4J_{\text{HH}} = 1.3$ Hz, 4 H, 17-H), 7.15 (t, $^3J_{\text{HH}} = 7.5$ Hz, 4 H, 18-H), 7.04 (tt, $^3J_{\text{HH}} = 7.3$, $^4J_{\text{HH}} = 1.4$ Hz, 2 H, 19-

H), 4.57 (s, 4 H, 15-H), 3.53–3.47 (m, 4 H, CH₂-N), 2.99–2.93 (m, 4 H, CH₂-N), 2.30–2.17 (m, 8 H, CH₂-N), 1.25–1.13 (m, 8 H, 3-H) ppm. ¹³C NMR (150 MHz, C₆D₆): $\delta = 155.8$ (2 C, C-1), 146.4 (2 C, C-16), 130.0 (4 C, C-17), 128.3 (4 C, C-18), 125.1 (2 C, C-19), 47.0 (4 C, CH₂-N), 40.2 (4 C, CH₂-N), 32.1 (2 C, C-15), 22.2 (4 C, C-3) ppm. ¹¹B NMR (128 MHz, C₆D₆): $\delta = 1.94$ (br. s, 2 B, B-S) ppm. MS (EI): $m/z = 544.2$ [C₂₈H₃₈B₂N₆S₂]⁺, 453.2 [C₂₁H₃₁B₂N₆S₂]⁺. HR-MS (EI): m/z (%) = 544.2766 (27), 543.2814 (12), 453.2233 (100), 452.2260 (51). IR (KBr): $\tilde{\nu} = 3055$ (w) (C-H_{arom} val.), 3023 (w) (C-H_{arom} val.), 2934 (m) (C-H_{aliph} val.), 2847 (m) (C-H_{aliph} val.), 1568 (s) (C=N val.), 1488 (w), 1456 (m), 1395 (w), 1366 (w), 1317 (m), 1275 (m), 1219 (m), 1178 (w), 1096 (w), 1041 (m) cm⁻¹. Crystal data for [BnSB(μ-hpp)]₂: C₂₈H₃₈B₂N₆S₂, $M_r = 544.39$, 0.16 × 0.15 × 0.10 mm³, monoclinic, space group $P2_1/c$, $a = 17.676(9)$, $b = 9.724(5)$, $c = 16.854(10)$ Å, $\beta = 106.437(8)^\circ$. $V = 2778(3)$ Å³, $Z = 4$, $d_{\text{calc}} = 1.301$ Mg m⁻³, Mo- K_α radiation (graphite-monochromated, $\lambda = 0.71073$ Å), $T = 100$ K, $\theta_{\text{range}} 2.40$ to 31.00° , reflections measd. 69297, indep. 8848, $R_{\text{int}} = 0.0730$, final R indices [$I > 2\sigma(I)$]: $R_1 = 0.0540$, $wR_2 = 0.1275$.

HB(μ-hpp)₂BBSBn: A Schlenk flask charged with [HB(μ-hpp)]₂ (105 mg, 0.35 mmol), dibenzyl disulfide (86 mg, 0.35 mmol) and toluene (10 mL) was heated to 90 °C for 3 h. After cooling to room temp., solid materials were filtered and the filtered solution was reduced to approx. a half of its volume. By addition of *n*-hexane (10 mL), a white solid precipitated. It was filtered again and crystals as colourless plates could be grown from the filtered solution by keeping it at room temp. for several days. The yield was not determined. C₂₁H₃₂B₂N₆S (422.21): calcd. C 59.74, H 7.64, B 5.12, N 19.91, S 7.59; found C 59.71, H 7.53, N 19.79. ¹H NMR (400 MHz, [D₈]THF): $\delta = 7.18$ (d, $^3J_{\text{HH}} = 7.5$ Hz, 2 H, 17-H), 7.04 (t, $^3J_{\text{HH}} = 7.4$ Hz, 2 H, 18-H), 6.93 (t, $^3J_{\text{HH}} = 6.9$ Hz, 1 H, 19-H), 3.52 (s, 2 H, 15-H), 3.37–2.83 (m, 16 H, CH₂-N), 1.95–1.37 (m, 8 H, 3-H, 6-H, 10-H, 13-H) ppm. ¹³C NMR (100 MHz, [D₈]THF): $\delta = 156.9$ (2 C, C-1), 147.8 (1 C, C-16), 130.1 (2 C, C-17), 128.0 (2 C, C-18), 125.1 (1 C, C-19), 48.2 (2 C, CH₂-N), 48.0 (2 C, CH₂-N), 46.0 (2 C, CH₂-N), 41.5 (2 C, CH₂-N), 35.5 (1 C, C-15), 23.9 (2 C, C-CH₂-C), 23.5 (2 C, C-CH₂-C) ppm. ¹¹B NMR (128 MHz, [D₈]THF): $\delta = 3.63$ (br. s, 1 B, B-S), -3.07 (br. s, 1B, B-H) ppm. MS (EI): $m/z = 422.3$ [C₂₁H₃₂B₂N₆S]⁺. IR (KBr): $\tilde{\nu} = 3050$ (w) (C-H_{arom} val.), 3027 (w) (C-H_{arom} val.), 2943 (m) (C-H_{aliph} val.), 2838 (s) (C-H_{aliph} val.), 2747 (w) (C-H_{aliph} val.), 2679 (w) (C-H_{aliph} val.), 2266 (m) (B-H val.), 1572 (s) (C=N val.), 1498 (w), 1452 (m), 1396 (w), 1363 (w), 1307 (s), 1274 (m), 1219 (s), 1178 (m), 1094 (m), 1045 (s) cm⁻¹. Crystal data for [HB(μ-hpp)₂BBSBn]: C₂₁H₃₂B₂N₆S, $M_r = 422.21$, 0.30 × 0.25 × 0.18 mm³, monoclinic, space group $P2(1)$, $a = 16.024(3)$, $b = 9.6990(19)$, $c = 15.467(3)$ Å, $\beta = 115.40(3)^\circ$. $V = 2171.5(7)$ Å³, $Z = 4$, $d_{\text{calc}} = 1.291$ Mg m⁻³, Mo- K_α radiation (graphite-monochromated, $\lambda = 0.71073$ Å), $T = 100$ K, $\theta_{\text{range}} 1.41$ to 27.48° , reflections measd. 15796, indep. 4933, $R_{\text{int}} = 0.0741$, final R indices [$I > 2\sigma(I)$]: $R_1 = 0.0601$, $wR_2 = 0.1435$.

UV/Vis Studies: Solutions of sulfur (0.18 mg, 0.75 μmol or 1.54 mg, 6.00 μmol) and [HB(μ-hpp)]₂ (1.80 mg, 6.00 μmol) in toluene (2.5 mL) were prepared separately and mixed immediately before starting the measurement. Then 3 mL of the solution were filled in a 1 cm quartz cell. The time measurements was started upon reaching the target temperature of 50 °C (ca 3 min after mixing). Measurements were carried out on a Varian Cary 5000 UV/Vis/NIR spectrophotometer equipped with a Specac 4000 High Stability Temperature Controller. The spectra were automatically baseline-corrected with the aid of the spectrum recorded for pure toluene.

X-ray Crystallographic Study: Suitable crystals were taken directly out of the mother liquor, immersed in perfluorinated polyether oil,

and fixed on top of a glass capillary. Measurements except for $[\text{BnSB}(\mu\text{-hpp})_2]_2$ were made on a Nonius-Kappa CCD diffractometer with low-temperature unit using graphite-monochromated Mo- K_α radiation. The temperature was set to 100 K. The data collected were processed using the standard Nonius software.^[41] All calculations were performed using the SHELXT-PLUS software package. Structures except for $[\text{BnSB}(\mu\text{-hpp})_2]_2$ were solved by direct methods with the SHELXS-97 program and refined with the SHELXL-97 program.^[42,43] Atomic coordinates and anisotropic thermal parameters of non-hydrogen atoms were refined by full-matrix least-squares calculations. Measurements of $[\text{BnSB}(\mu\text{-hpp})_2]_2$ were made on a Bruker AXS Smart 1000 CCD diffractometer. The structure was solved by the charge flip procedure^[44,45] and refined by full-matrix least-squares methods based on F^2 against all unique reflections. All non-hydrogen atoms were given anisotropic displacement parameters. Hydrogen atoms were input at calculated positions and refined with a riding model.^[46,39] Graphical handling of all structural data during solution and refinement was performed with XPMA.^[47]

CCDC-779080 {for $[\text{HB}(\mu\text{-hpp})_2(\mu\text{-S})]$ }, 779078 {for $[\text{PhSB}(\mu\text{-hpp})_2]$ }, 779077 {for $[\text{HB}(\mu\text{-hpp})_2\text{BSPH}]$ }, 779076 {for $[\text{BnSB}(\mu\text{-hpp})_2]$ }, 779079 {for $[\text{HB}(\mu\text{-hpp})_2\text{BSBn}]$ } and 780574 {for $[\text{HB}(\mu\text{-hpp})_2(\mu\text{-S})]$ } contain the supplementary crystallographic data for this paper. These data can be obtained free of charge from The Cambridge Crystallographic Data Centre via www.ccdc.cam.ac.uk/data_request/cif.

Computational Details: Quantum chemical calculations were carried out with the TURBOMOLE V.5–9.1 program package.^[48] The BP86 functional^[49] in combination with the def2-SV(P) basis set^[50] and the appropriate auxiliary basis set^[51] for RI-J calculations was used.

Supporting Information (see also the footnote on the first page of this article): Photographs of the solution at different stages of the reaction between $[\text{HB}(\mu\text{-hpp})_2]_2$ and S_8 , summary of the results of the quantum chemical calculations.

Acknowledgments

The authors thank the Deutsche Forschungsgemeinschaft (DFG) for continuous financial support. Nikola Schulenberg thanks the Landesgraduiertenförderung (LGF) (Funding Program of the state of Baden-Württemberg) for a PhD grant.

- [1] Y. Wang, B. Quillian, P. Wie, C. S. Wannere, Y. Xie, R. B. King, H. F. Schaefer III, P. von Rague Schleyer, G. H. Robinson, *J. Am. Chem. Soc.* **2007**, *129*, 12412–12413.
- [2] D. Scheschkewitz, *Angew. Chem. Int. Ed.* **2008**, *47*, 1995–1997.
- [3] Y. Segawa, M. Yamashita, K. Nozaki, *Science* **2006**, *314*, 113–115.
- [4] T. B. Marder, *Science* **2006**, *314*, 69–70.
- [5] H. Braunschweig, C.-W. Chiu, K. Radacki, T. Kupfer, *Angew. Chem. Int. Ed.* **2010**, *49*, 2041–2044.
- [6] K. Nozaki, *Nature* **2010**, *464*, 1136–1137.
- [7] H. Braunschweig, R. D. Dewhurst, A. Schneider, *Chem. Rev.* **2010**, in press (10.1021/cr900333n), and references cited therein.
- [8] L. Dang, Z. Lin, T. B. Marder, *Chem. Commun.* **2009**, 3987–3995.
- [9] H. Braunschweig, K. Radacki, A. Schneider, *Science* **2010**, *328*, 345–347.
- [10] C. W. Hamilton, R. T. Baker, A. Staubitz, I. Manners, *Chem. Soc. Rev.* **2009**, *38*, 279–293.
- [11] G. C. Welch, R. R. San Juan, J. D. Masuda, D. W. Stephan, *Science* **2006**, *314*, 1124–1126.
- [12] G. C. Welch, D. W. Stephan, *J. Am. Chem. Soc.* **2007**, *129*, 1880–1881.
- [13] M. A. Dureen, G. C. Welch, T. M. Gilbert, D. W. Stephan, *Inorg. Chem.* **2009**, *48*, 9910–9917.
- [14] O. Ciobanu, P. Roquette, S. Leingang, H. Wadepohl, J. Mautz, H.-J. Himmel, *Eur. J. Inorg. Chem.* **2007**, 4530–4534.
- [15] O. Ciobanu, F. Allouti, P. Roquette, S. Leingang, M. Enders, H. Wadepohl, H.-J. Himmel, *Eur. J. Inorg. Chem.* **2008**, 5482–5493.
- [16] O. Ciobanu, E. Kaifer, H.-J. Himmel, *Angew. Chem.* **2009**, *48*, 5646–5649; *Angew. Chem. Int. Ed.* **2009**, *121*, 5538–5541.
- [17] R. Dinda, O. Ciobanu, H. Wadepohl, O. Hübner, R. Acharya, H.-J. Himmel, *Angew. Chem.* **2007**, *119*, 9270–9273; *Angew. Chem. Int. Ed.* **2007**, *46*, 9110–9113.
- [18] O. Ciobanu, A. Fuchs, M. Reinmuth, A. Lebkücher, E. Kaifer, H.-J. Himmel, *Z. Anorg. Allg. Chem.* **2010**, *636*, 543–550.
- [19] O. Ciobanu, D. Emeljanenko, E. Kaifer, H.-J. Himmel, *Inorg. Chem.* **2008**, *47*, 4774–4778.
- [20] N. Schulenberg, M. Jäkel, E. Kaifer, H.-J. Himmel, *Eur. J. Inorg. Chem.* **2009**, 4809–4819.
- [21] G. Robinson, C. Y. Tang, R. Köppe, A. R. Cowley, H.-J. Himmel, *Chem. Eur. J.* **2007**, *13*, 2648–2654.
- [22] O. Ciobanu, H.-J. Himmel, *Eur. J. Inorg. Chem.* **2007**, 3565–3572.
- [23] F. A. Cotton, C. A. Murillo, X. Wang, C. C. Wilkinson, *Inorg. Chem.* **2006**, *45*, 5493–5500.
- [24] F. A. Cotton, C. A. Murillo, X. Wang, C. C. Wilkinson, *Dalton Trans.* **2006**, 4623–4631.
- [25] We showed in the past that the H_2 can be added to the element-element bond of the group 13 element dimer Ga_2 with only small activation barrier (30–50 kJ mol^{-1}). See: a) H.-J. Himmel, L. Manceron, A. J. Downs, P. Pullumbi, *Angew. Chem.* **2002**, *114*, 829–832; *Angew. Chem. Int. Ed.* **2002**, *41*, 796–799; b) H.-J. Himmel, L. Manceron, A. J. Downs, P. Pullumbi, *J. Am. Chem. Soc.* **2002**, *124*, 4448–4457; c) A. Köhn, H.-J. Himmel, B. Gaertner, *Chem. Eur. J.* **2003**, *9*, 3909–3919.
- [26] a) Y. Chen, J. L. Fulton, J. C. Linehan, T. Autrey, *J. Am. Chem. Soc.* **2005**, *127*, 3254–3255; b) J. L. Fulton, J. C. Linehan, T. Autrey, M. Balasubramanian, Y. Chen, N. K. Szymczak, *J. Am. Chem. Soc.* **2007**, *129*, 11936–11949.
- [27] a) C. A. Jaska, K. Temple, A. J. Lough, I. Manners, *Chem. Commun.* **2001**, 962–963; b) C. A. Jaska, K. Temple, A. J. Lough, I. Manners, *J. Am. Chem. Soc.* **2003**, *125*, 9424–9434; c) C. A. Jaska, I. Manners, *J. Am. Chem. Soc.* **2004**, *126*, 9776–9785.
- [28] Y. D. Blum, R. M. Laine, US Pat., 4801439, **1989**.
- [29] If less than 10% of the complex is added, the reaction takes some more time for completion.
- [30] R. J. Keaton, J. M. Blacquiere, R. T. Baker, *J. Am. Chem. Soc.* **2007**, *129*, 1844–1845.
- [31] For a recent mechanistical study on the basis of quantum chemical calculations, see: P. M. Zimmerman, A. Paul, C. B. Musgrave, *Inorg. Chem.* **2009**, *48*, 5418–5433.
- [32] O. Ciobanu, F. Allouti, P. Roquette, S. Leingang, M. Enders, H. Wadepohl, H.-J. Himmel, *Eur. J. Inorg. Chem.* **2008**, 5482–5493.
- [33] Photoelectron spectroscopic studies on $\text{B}(\text{SMe})_3$, $\text{MeB}(\text{SMe})_2$ and Me_2BSMe showed an increasing π -bond character, see: J. Kroner, D. Nölle, H. Nöth, *Z. Naturforsch., Teil B* **1973**, *28*, 416.
- [34] H. Fußstetter, H. Nöth, K. Peters, H. G. von Schnering, J. C. Huffman, *Chem. Ber.* **1980**, *113*, 3881–3890.
- [35] H. Nöth, R. Ullmann, *Chem. Ber.* **1975**, *108*, 3125–3131.
- [36] P. Greiwe, V. Beez, H. Pritzkow, W. Siebert, *Eur. J. Inorg. Chem.* **2001**, 381–386.
- [37] D. Männig, C. K. Narula, H. Nöth, V. Wietelmann, *Chem. Ber.* **1985**, *118*, 3748–3758.
- [38] R. Bonnaterre, G. Cauquis, *J. Chem. Soc., Chem. Commun.* **1972**, 293–294.

- [39] R. P. Martin, W. H. Doub, J. L. Roberts, D. T. Sawyer, *Inorg. Chem.* **1973**, *12*, 1921–1925.
- [40] V. Pinon, J. P. Lelieur, *Inorg. Chem.* **1991**, *30*, 2260–2264.
- [41] DENZO-SMN, Data processing software, Nonius **1998**; <http://www.nonius.com>.
- [42] a) G. M. Sheldrick, *SHELXS-97, Program for Crystal Structure Solution*, University of Göttingen, **1997**; <http://shelx.uni-ac.gwdg.de/SHELX/index.html>; b) G. M. Sheldrick, *SHELXL-97, Program for Crystal Structure Refinement*, University of Göttingen, **1997**; <http://shelx.uni-ac.gwdg.de/SHELX/index.html>.
- [43] *International Tables for X-ray Crystallography*, vol. 4, Kynoch Press, Birmingham, U.K., **1974**.
- [44] a) G. Oszlányi, A. Sütő, *Acta Crystallogr., Sect. A* **2004**, *60*, 134–141; b) G. Oszlányi, A. Sütő, *Acta Crystallogr., Sect. A* **2005**, *61*, 147–152.
- [45] L. Palatinus, *SUPERFLIP*, EPF Lausanne, Switzerland, **2007**; L. Palatinus, G. Chapuis, *J. Appl. Crystallogr.* **2007**, *40*, 786–790.
- [46] G. M. Sheldrick, *Acta Crystallogr., Sect. A* **2008**, *64*, 112–122.
- [47] L. Zsolnai, G. Huttner, *XPMA*, University of Heidelberg, **1994**, <http://www.uni-heidelberg.de/institute/fak12/AC/huttner/software/software.html>.
- [48] a) O. Treutler, R. Ahlrichs, *J. Chem. Phys.* **1995**, *102*, 346–354; b) M. v. Arnim, R. Ahlrichs, *J. Comput. Chem.* **1998**, *19*, 1746–1757; c) M. Haeser, R. Ahlrichs, *Chem. Phys. Lett.* **1995**, *242*, 652–660.
- [49] a) P. A. M. Dirac, *Proc. R. Soc. (London) A* **1929**, *123*, 714–733; b) J. C. Slater, *Phys. Rev.* **1951**, *81*, 385–390; c) S. H. Vosko, L. Wilk, M. Nusair, *Can. J. Phys.* **1980**, *58*, 1200–1211; d) A. D. Becke, *Phys. Rev. A* **1988**, *38*, 3098–3100; e) J. P. Perdew, *Phys. Rev. B* **1986**, *33*, 8822–8824.
- [50] F. Weigend, R. Ahlrichs, *Phys. Chem. Chem. Phys.* **2005**, *7*, 3297–3305.
- [51] F. Weigend, *Phys. Chem. Chem. Phys.* **2006**, *8*, 1057–1065.

Received: May 28, 2010

Published Online: August 24, 2010